

Cite this article as: Gao Changqi, Ma Qin, Wei Yupeng, et al. Interfacial Microstructure and Mechanical Properties of Basalt Fibers Reinforced Aluminium Matrix Composites Optimized by Ni-Co-P Intermediate Layer[J]. Rare Metal Materials and Engineering, 2023, 52(12): 4013-4020. DOI: 10.12442/j.issn.1002-185X.E20230014.

ARTICLE

Interfacial Microstructure and Mechanical Properties of Basalt Fibers Reinforced Aluminium Matrix Composites Optimized by Ni-Co-P Intermediate Layer

Gao Changqi^{1,2}, Ma Qin^{1,2,3}, Wei Yupeng^{1,2}, Tian Jiangxia^{1,2}, Wang Qiaobo^{1,2}, Wei Mingyu^{1,2}, Ren Xiaohu^{1,2}, Ding Yusheng^{1,2}

¹ State Key Laboratory of Advanced Processing and Recycling of Nonferrous Metals, Lanzhou University of Technology, Lanzhou 730050, China; ² School of Materials Science and Engineering, Lanzhou University of Technology, Lanzhou 730050, China; ³ School of Mechanical and Electronic Engineering, Quanzhou University of Information Engineering, Quanzhou 362000, China

Abstract: Interface optimization is an effective way to improve the performance of aluminum matrix composites. Basalt fibers (BF) modified by Ni-Co-P alloy coatings with about 0.2 μm in thickness were prepared by electroless plating firstly, and then Ni-Co-P coated basalt fibers reinforced 2024Al matrix composites (BF(Ni-Co-P)/Al) and uncoated basalt fibers reinforced 2024Al matrix composites (BF/Al) were fabricated by vacuum hot pressing sintering process. The effects of Ni-Co-P coatings on the interface microstructure and tensile properties of BF(Ni-Co-P)/Al composites were studied. The results show that stable Ni-Co-P intermediate layer is formed in BF(Ni-Co-P)/Al composites, which can not only restrain harmful interface reaction but also optimize the interface bonding state between matrix and basalt fiber. The density and hardness of BF(Ni-Co-P)/Al composites are superior to those of BF/Al composites, and yield strength (252 MPa) and ultimate tensile strength (360 MPa) of BF(Ni-Co-P)/Al composites with basalt fibers content of 30vol% have a significant improvement compared with those of BF/Al composites and 2024Al matrix, and the fracture mode is progressive accumulative failure.

Key words: Ni-Co-P coated basalt fibers; Al matrix composites; interface microstructure; mechanical properties

As one of the high performance fibers, basalt fibers possess excellent performances such as a wide applicable temperature range from $-269\text{ }^{\circ}\text{C}$ to $-700\text{ }^{\circ}\text{C}$ ^[1], high specific strength and modulus^[2], good chemical stability and corrosion resistance^[3], so they have a wide application prospect in the fields of dielectric materials, structural materials, sound insulation materials, etc^[4-5]. Particularly, in a non-vacuum environment of high temperature ($\geq 600\text{ }^{\circ}\text{C}$), basalt fibers have the highest residual strength and the lowest mass loss rate compared with other high performance fibers like carbon fibers, ultra-high molecular weight polyethylene fibers and aramid fibers^[3,6]. More importantly, basalt fibers are environment-friendly materials because of degradability and low manufacturing cost and energy consumption^[7]. The application of basalt fibers on the composite strengthening and toughening of lightweight

alloy can reduce manufacturing cost and broaden the application prospects in both civil and military fields of lightweight and high strength metal matrix composites^[5,8].

Currently, the researches about the performances of basalt fibers reinforced metals matrix composites have been reported. The research of Karthigeyan R et al^[9-10] indicated that the tribological behavior, coefficient of thermal expansion (CTE) and tensile properties of short basalt fibers (BF) reinforced aluminium matrix composites fabricated by stir casting process are obviously superior to those of matrix alloys, while relationship between interface and performance was not studied. Xie et al^[11] studied the interface microstructure and mechanical properties of basalt fibers reinforced aluminum matrix composites (BF/Al) fabricated by vacuum pressure infiltration method, and the results showed that alumina oxide

Received date: May 16, 2023

Foundation item: National Natural Science Foundation of China (52262012); Innovation Fund Project of Gansu Provincial Department of Education (2021A-030)

Corresponding author: Ma Qin, Ph. D., Professor, School of Materials Science and Engineering, Lanzhou University of Technology, Lanzhou 730050, P. R. China, E-mail: maq@lut.cn

Copyright © 2023, Northwest Institute for Nonferrous Metal Research. Published by Science Press. All rights reserved.

amorphous reaction layer is generated at the interface owing to the redox reaction between silicon dioxide of basalt fibers and Al matrix, and the bending properties of BF/Al composites were not improved. Also, the research about interface structure between basalt whiskers and A356 aluminium matrix and tensile strength of composites was reported by Onuh et al^[12]. They found that metastable Al-Si-Ca intermetallic compounds and stable Al-Fe-Si-Mn intermetallic compounds are produced between basalt whiskers and A356 aluminium matrix, which can guarantee the load transfer from matrix to reinforcements, but the tensile strength of BF/Al only has a smaller improvement compared with that of A356 aluminium. Interestingly, the mechanical properties of BF/Al composites did not have an obvious improvement compared with that of alloy matrix, which were caused by the harmful interface reaction and fibers damage due to the phase transition of BFs in the preparation of composite materials. According to the principles of thermodynamics and dynamics^[13-14], interfacial reaction and fibers phase transition can be effectively inhibited by the methods such as decreasing preparation temperature and shortening holding time. Akhlaghi et al^[15] proposed a new method to fabricate BF/Al composites, which can significantly shorten holding time of composites and reduce the degradation of fiber properties. The process is as follows: firstly, aluminium coated BFs were prepared by the immersion of fibers in molten aluminium at 600±5 °C for 2 s, and then the BF/Al composites were fabricated by the sintering of aluminium coated BFs under the sintering pressure of 630 MPa at 300 °C for 7 min. However, the measured values of ultimate tensile strength were completely inconsistent with the theoretical value owing to the defects in composites, which were produced by the improper infiltration of fiber bundles with too short immersion time. Besides, the effects of infiltration temperature on the mechanical properties of BF/Al composites and tensile strength of basalt fibers were discussed^[16]. Fully dense BF/Al composites with no obvious interface reaction can be obtained by vacuum pressure infiltration under 10 MPa at 660 °C for 10 min, while the mechanical properties have no increase compared with Ref. [12] owing to non-ideal distribution of reinforcement in matrix and decrease in inherent strength of fibers caused by the decomposition of surface treatment agents. Furthermore, Yang et al^[17] studied the effects of reinforcement content on the mechanical properties of short basalt fibers reinforced Al matrix composites fabricated by hot-press sintering method and found that the mechanical properties of composites decrease when the fibers content exceeds 10wt% . Unfortunately, mechanical properties of BF/Al composites, having a large gap with theoretical value, were greatly inferior to those of carbon fibers reinforced aluminium matrix composites (CF/Al)^[18-19], and it is of great significance to further improve the properties of BF/Al composites for the preparation of high performance and low cost Al matrix composites. Metallization modification of fibers surface not only inhibits the element interdiffusion between reinforcement and metal matrix but also improves the interface compatibility

and wettability of composites, which has been widely used for the interface optimization of CF/Al composites^[20-22]. Regrettably, interface optimization by metallization modification of fibers in basalt fiber reinforced Al matrix composites was seldom reported.

In this work, the thickness-controlled nickel-cobalt-phosphorus (Ni-Co-P) complex alloy coatings were deposited on the surface of basalt fibers by electroless plating firstly, and then aluminium matrix composites reinforced by Ni-Co-P coated basalt fibers and uncoated basalt fibers were fabricated by vacuum hot pressing sintering under the pressure of 90 MPa at 490 °C for 10 min. The effects of Ni-Co-P intermediate layer on the microstructures and mechanical properties of BF/Al composites were investigated by the comparison of different composites. Moreover, the tensile failure mechanisms of the composites were analyzed.

1 Experiment

The basalt fibers (BFs) as reinforcements were provided by Jiangsu Tianlong continuous basalt fiber Co., Ltd, China, and performance parameters are shown in Table 1. 2024Al powders provided by Hebei Qinbang New Material Technology Co., Ltd, China were used as the metal matrix.

Before the deposition of Ni-Co-P alloy coatings, BFs were immersed in 50 g/L NaOH solution for 10 min to remove surface impurities and contaminants. The fabrication procedure of Ni-Co-P coated BFs is shown in Fig. 1. Firstly, BFs were sensitized by the adsorption of Sn²⁺ ions on the surface through impregnation of HCl (40 ml/L) and SnCl₂ (10 g/L) mixed solutions, and then washed several times by distilled water. Secondly, the sensitized BFs were activated by the Pd atoms adsorbed on surface caused by reduction of Sn²⁺ in the activating agent consisting of 0.5 g/L PdCl₂ and 20 ml/L HCl. Then the active fibers were rinsed by distilled water. After sensitization and activation, the Ni-Co-P coatings with different thicknesses were deposited on BFs surface by electroless plating at the constant temperature of 70 °C and held by thermostat water bath cauldron for 0, 5, 10, 15 and 20 min, and the composition and pH of electroless plating solution are shown in Table 2. At the end of holding time, Ni-Co-P coated basalt fibers were cleaned by distilled water and dried at 60 °C for 8 h in a vacuum drying closet.

Based on the comparison of thickness and integrity of Ni-Co-P coatings, the Ni-Co-P coated basalt fibers deposited for 10 min were used to reinforce 2024Al matrix composites. The fabrication process of BFs reinforced 2024Al matrix composites is as follows. Firstly, BFs were woven into preforms and filled by the 2024Al/alcohol suspension liquid with the volume ratio of 1: 30 by vacuum filtration. Afterwards, the filled preforms were placed in a graphite mould and dried at 45 °C by the vacuum drying closet. Lastly, the Al

Table 1 Performance parameters of basalt fibers

Performance	$R_m/\times 10^3\text{MPa}$	E/GPa	$\delta/\%$	$\rho/\text{g}\cdot\text{cm}^{-3}$	$D/\mu\text{m}$
Value	2.61	81	3.8	2.7	7

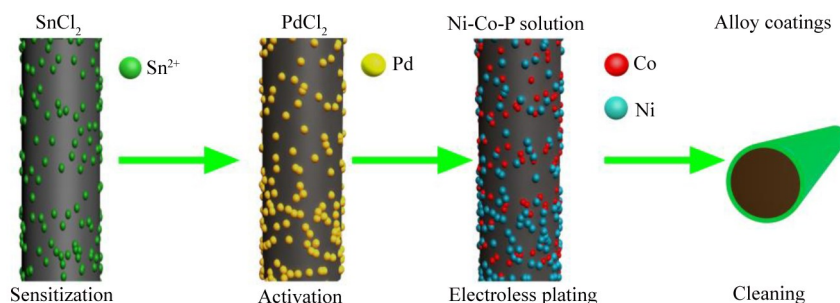


Fig.1 Electroless plating procedure of Ni-Co-P coatings on BFs

Table 2 Composition of Ni-Co-P electroless plating solution

Component	Content/g·L ⁻¹	Function
Nickel sulfate	12.08	Main salt
Cobalt sulfate	12.92	Main salt
Sodium citrate	40.00	Complexing agent
Ammonium sulfate	40.00	Buffer
Sodium hypophosphite	20.00	Reducing agent
Sodium hydroxide	-	pH adjusting (8.9±0.05)

matrix composites were fabricated by the vacuum hot pressing sintering under 90 MPa at 490 °C for 10 min. The uncoated BF reinforced 2024Al matrix composites (BF/Al) and Ni-Co-P coated BF reinforced 2024Al matrix composites (BF(Ni-Co-P)/Al) with fibers volume fraction of 10vol%, 20vol%, 30vol% and 40vol% were obtained by the regulation of volume ratio of reinforcement in matrix.

The phases of uncoated BF and BF modified with Ni-Co-P coatings were examined by X-ray diffractometer (D8 advance XRD, Germany). The scanning electron microscope (SEM, JSM-6700F, Japan) equipped with energy dispersive spectrometer (EDS) was used to investigate microstructure morphology and elemental composition of Ni-Co-P coatings and Al matrix composites. Interface microstructure and element distribution of BF(Ni-Co-P)/Al composites were observed by the transmission electron microscope (JEOL-200CX, Japan). The composites samples were processed into tensile specimen with gauge length of 10 mm using wire-electrode cutting, and then polished by 1000# waterproof sandpaper to remove the processing tool marks. The tensile properties of all the samples were tested using electronic universal testing machine (E44.304 MTS, USA) with the constant tensile speed of 0.2 mm/min. Lastly, the fractures of different composites were characterized by SEM.

2 Results and Discussion

2.1 XRD of basalt fibers and Ni-Co-P coated basalt fibers

The phases of uncoated BF and Ni-Co-P coated BF deposited for 10 min are shown in Fig.2. Clearly, there are no obvious sharp diffraction peaks in spectra of uncoated BF, while the broad and weak diffuse reflection peak is observed at 20°–30° (2θ), which may be caused by amorphous phase structure of basalt fibers. After Ni-Co-P coatings modification,

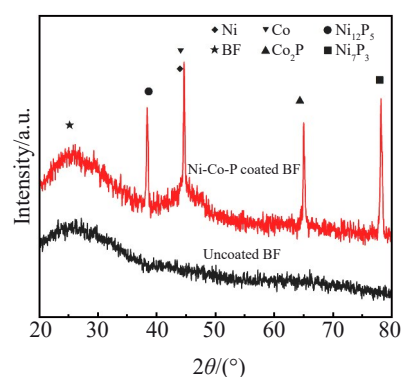


Fig.2 XRD patterns of uncoated BF and Ni-Co-P coated BF

some sharp diffraction peaks of Ni₁₂P₅ (38.5°), Ni-Co (44.7°), Co₂P (65°) and Ni₃P₂ (78°) are observed in spectra of Ni-Co-P coated BF. Diffuse reflection peaks of Ni and Co are difficult to distinguish because of their similar atomic radius and lattice constant. Interestingly, the element P exists in the form of nickel phosphide and cobalt phosphate compounds instead of simple substance owing to the co-deposition of Ni, Co and P atoms.

2.2 Effects of deposition time on microstructure of Ni-Co-P coatings

To investigate the variation of microstructure of Ni-Co-P coatings with the deposition time, the morphologies of Ni-Co-P coatings with different deposition time of 5, 10, 15 and 20 min are shown in Fig.3. As seen in Fig.3a, uncoated basalt fibers with uniform diameter of about 7 μm have a smooth surface, and no obvious defects exist. After deposition for 5 min, the Ni-Co-P coatings on BF have a flat and compact surface (Fig.3b), while the local areas of fiber surface are exposed because of poor coatings integrality. When the deposition time increases to 10 min, the integrality and compactness of Ni-Co-P coatings (as shown in Fig.3c) improve obviously and a few Ni-Co-P cellular particles are generated. With further extending the deposition time, the amount of Ni-Co-P cellular particles are obviously increased and particle sizes become larger than those of coatings deposited for 10 min, as shown in Fig.3d and 3e. In summary, the microstructure of Ni-Co-P coatings with 10 min deposition time is superior to others, and the thickness is up to about 0.3 μm. Besides, the content of elements Ni, Co and P is

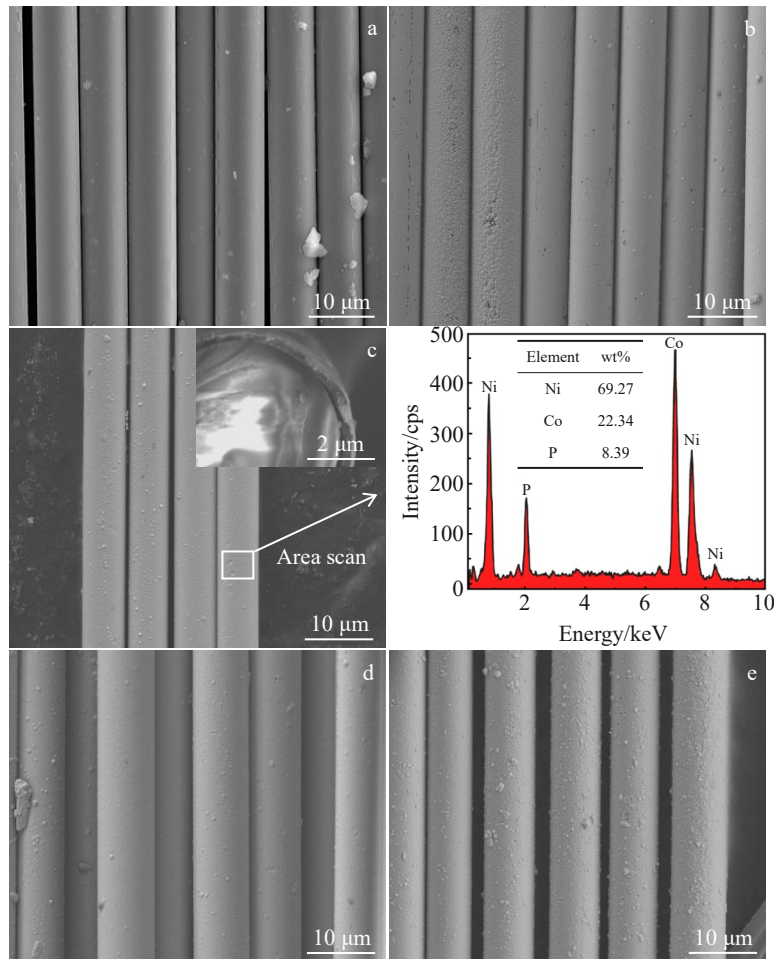
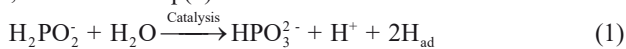


Fig.3 Morphologies of uncoated basalt fibers (a) and Ni-Co-P coated basalt fibers with deposition time of 5 min (b), 10 min (c), 15 min (d) and 20 min (e); EDS analysis results of the scanning area with deposition time of 10 min

69.27wt%, 22.34wt% and 8.39wt%. The microstructure and composition of Ni-Co-P coatings are affected by the deposition mechanism of element Ni and Co. In the process of electroless plating, active hydrogen atoms (H_{ad}) are generated by hydrolysis reaction of hypophosphite under the catalysis of Pd, as shown in Eq.(1)^[23]:



Majority of H_{ad} react with nickel ions (Ni^{2+}) and cobalt ions (Co^{2+}) to produce Ni atoms and Co atoms (Eq.(2) and Eq.(3)), and then absorb on fiber surface in the form of atomic clusters^[24], which is the reasons for the formation of Ni-Co-P cellular particles. Notably, the standard electrode potential ($E^\ominus = -0.25$ V) of element Ni is greater than that of Co ($E^\ominus = -0.277$ V), so the producing rate of nickel atoms is significantly higher than that of cobalt atoms. Therefore, the Ni content in Ni-Co-P coatings is higher than Co content. Besides, a small amount of H_{ad} atoms react with hypophosphite to induce the co-deposition of P and metal particles, which is the main reason for the formation of nickel phosphide and cobalt phosphate compounds.

2.3 Interface microstructure of BF(Ni-Co-P)/Al composites

The HAADF image and element distribution of interface of 2024Al matrix composites reinforced by Ni-Co-P coated basalt fibers prepared with 10 min deposition time are shown in Fig.4. As shown in HAADF image, highlight areas reflect that elements Ni, Co and P with high atomic numbers are distributed between Al matrix and basalt fibers, and an obvious intermediate layer with a thickness of about 160 nm forms, which is consistent with Ni-Co-P coating thickness. According to element mappings of Al and Mg, elements have no obvious diffusion to Ni-Co-P intermediate layer, indicating that alloy intermediate layer protects the basalt fiber from the reaction with 2024Al matrix. As can be seen from HAADF image and element distribution of O and Si, there is a remarkable interface formed between Ni-Co-P intermediate layer and BFs. The element distribution is affected by the mixing enthalpy of each element. According to Boltzmann's hypothesis^[25-26], mixing enthalpy of Al-Co and Al-Ni (-19 and -22 kJ/mol) is higher than that of Ni-Co (0 kJ/mol), which means that Ni and Co can form stable solid solution phase so that element Al cannot diffuse to the Ni-Co-P coatings and react with BFs. Similarly, the value of mixing enthalpy of Mg-

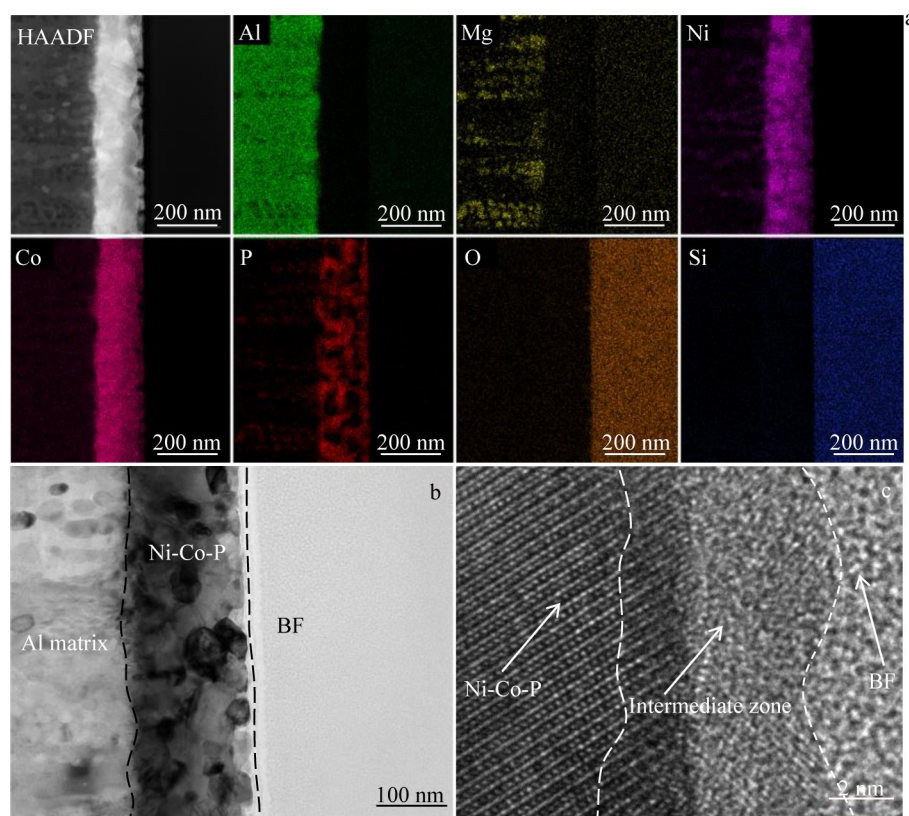


Fig.4 HAADF image and the element distribution of interface between basalt fibers and Al matrix (a), TEM image of interface of BF(Ni-Co-P)/Al composites (b), and HRTEM image of interface between basalt fibers and Ni-Co-P coatings (c)

Co is 3 kJ/mol, and diffusion and reaction of Mg with Ni-Co-P coatings are inhibited.

The microstructure of interface of BF(Ni-Co-P)/Al composites is shown in Fig.4a. Obvious interfaces are formed between basalt fibers and Ni-Co-P intermediate layer, Ni-Co-P intermediate layer and Al matrix, consistent with HAADF image and element distribution. While dislocations are not generated near the interface, indicating that existence of Ni-Co-P intermediate layer improves the compatibility of thermal expansion coefficient between Al matrix and BFs. Interestingly, the intermediate zone with lattice mismatch with the thickness of 3 nm is formed between Ni-Co-P intermediate layer and BFs (Fig.4c), which is conducive to load transfer. In addition, amorphous structures of BFs indicate that BFs are not damaged by Ni-Co-P intermediate layer.

2.4 Density of BF(Ni-Co-P)/Al composites

The density of composites can reflect the lightweight effect of reinforcement. The theoretical density can be calculated according to Eq.(4):

$$\rho_c = \rho_m V_m + \rho_r V_r \quad (4)$$

where ρ_c , ρ_m and ρ_r mean density value of composites, matrix (2.81g/cm³) and reinforcement (2.63 g/cm³), respectively; V_r and V_m refer to the volume fraction of reinforcement and matrix, respectively. After calculation, the theoretical density of BF/Al composites and BF(Ni-Co-P)/Al composites with different BFs volume fractions is shown in Fig.5. For BF/Al composites, the values of measured density are lower than

theoretical density, and they have the same variation from high to low with the increase in BF volume fraction, as shown in Fig.5a. Interestingly, the theoretical density of BF(Ni-Co-P)/Al composites increases with improvement of BF volume fraction, while the measured density increases first, then reduces, and reaches the maximum value when the BF volume fraction is up to 30vol%. The difference of density variation between BF/Al composites and BF(Ni-Co-P)/Al composites is mainly caused by the presence of Ni-Co-P coatings. Ni-Co-P coatings not only improve the wettability and compatibility between matrix and BFs but also fill the fiber bundles, which can efficiently inhibit the generation of cavity defects between BFs. Besides, the lightweight effects of BFs are restrained in BF(Ni-Co-P)/Al composites because the density of Ni-Co-P coatings is larger than that of 2024Al matrix and BFs. Therefore, the measured density of BF(Ni-Co-P)/Al composites is closer to the theoretical value. In other words, BF(Ni-Co-P)/Al composites is denser than BF/Al composites under the same BFs volume fraction conditions.

2.5 Hardness of BF(Ni-Co-P)/Al composites

The variations in hardness of BF/Al composites and BF(Ni-Co-P)/Al composites with different BFs content are shown in Fig.6. With the increase in BFs, the hardness increases firstly and then decreases, and the maximum values of BF/Al and BF(Ni-Co-P)/Al composites are up to 60 HRB and 72 HRB, respectively, higher than the maximum value of 2024Al. The hardness of BF(Ni-Co-P)/Al composites is superior to that of

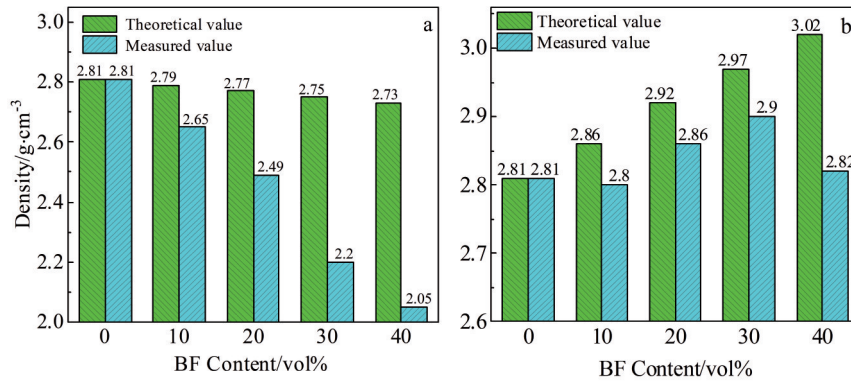


Fig.5 Theoretical density and measured density of BF/Al composites (a) and BF(Ni-Co-P)/Al composites (b)

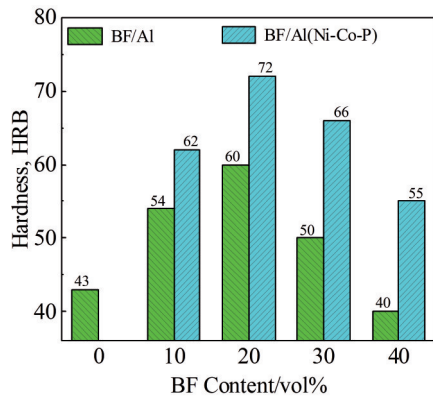


Fig.6 Hardness of BF/Al composites and BF(Ni-Co-P)/Al composites

BF/Al composites owing to the optimization of Ni-Co-P coatings. Ni-Co-P coatings inhibit the generation of cavity

defect among fiber bundles while form Ni-Co solid solution so that the deformation resistance is improved. Besides, the excessive fiber content can cause the generation of cavity defects, so the hardness of composites with 40vol% BFs is lower than that of others.

2.6 Tensile properties and failure behavior of BF(Ni-Co-P)/Al composites

The tensile properties of BF/Al composites and BF(Ni-Co-P)/Al composites with 0vol%, 10vol%, 20vol%, 30vol%, and 40vol% BF are shown in Fig.7a and 7b, respectively. Clearly, the yield strength (YS) and ultimate tensile strength (UTS) of composites increase first and then decrease with the improvement of BFs content, while the elongation (EL) decreases. The YS and UTS of BF/Al composites reach the maximum of 94 and 238 MPa, respectively when BFs content is up to 10vol% , while YS and UTS of BF(Ni-Co-P)/Al composites reach the maximum of 252 and 360 MPa,

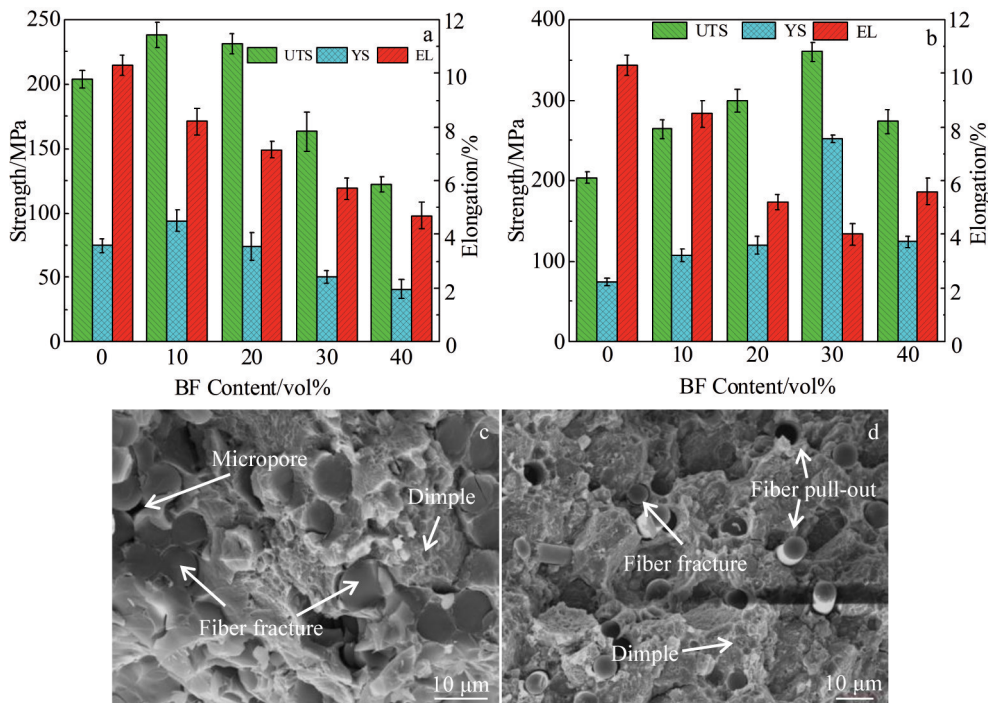


Fig.7 Tensile properties (a-b) and fracture morphologies (c-d) of BF/Al composites (a, c) and BF(Ni-Co-P)/Al composites (b, d)

respectively when the BF content is up to 30vol%. Compared with those of 2024Al matrix, YS and UTS of BF(Ni-Co-P)/Al composites are increased by 240% and 76%, respectively, and EL is decreased by 40.9%.

Compared with those of BF/Al composites, YS and UTS of BF(Ni-Co-P)/Al composites have higher improvement, which is attributed to the presence of Ni-Co-P intermediate layer. As observed from the fracture morphology of BF/Al composites (Fig. 7c), the dimples on Al matrix indicate that the failure mechanism of Al matrix composites is not affected by the reinforcement, while basalt fibers fracture simultaneously with the matrix. Also, the micropores are formed between fibers due to inadequate filling of Al, and this may become the crack source. According to the Ref. [17], the reactions between basalt fibers and Al matrix occur, as shown in Eq.(5) and Eq.(6):



On the one hand, metallurgical bonding interface generated by the above reactions improves the load transfer from matrix to basalt fibers. On the other hand, interface reaction destroys the intrinsic structure of BFs so that the load-bearing effect of fibers is difficult to exert. The microcracks initiate at the interface and easily propagate into the fiber interior. Consequently, BF/Al composites is of brittle fracture and their tensile properties decrease with the increase in BF content, which is inconsistent with variation of the theoretical strength calculated by rule of mixture of composites. For BF(Ni-Co-P)/Al composites, Ni-Co-P intermediate layers not only restrain formation of cavity defects and interface reaction between basalt fibers and Al matrix, but also improve the load transfer by adjusting the interface bonding. In the tensile process, microcracks initiate in the matrix firstly, and then propagate to interface and deflect so that fracture and pull-out of fibers appear simultaneously. As shown in Fig.7d, some basalt fibers are pull-out, which are conducive to the EL of composites by the crack-bridging toughening. Other composites fail on the surface of fracture, and they have excellent load-bearing effect. Therefore, the tensile properties of BF(Ni-Co-P)/Al composites improve obviously and it exhibits progressive cumulative failure mode.

3 Conclusions

1) Ni-Co-P coatings can be deposited on the surface of basalt fibers and used to form stable Ni-Co-P intermediate layer to optimize the interface of basalt fibers reinforced 2024Al matrix composites by the inhibition of interface reaction and improvement of interface state between basalt fibers and Al alloy matrix.

2) The yield strength and ultimate tensile strength of BF(Ni-Co-P)/Al composites can reach to 252 and 360 MPa, respectively, which are higher than those of BF/Al composites and 2024Al matrix.

3) Owing to the presence of Ni-Co-P intermediate layer, the failure mode of basalt fibers reinforced 2024Al matrix

composites changes from brittle fracture to progressive cumulative failure.

References

- 1 Fabrizio Sarasini, Jacopo Tirillo, Maria Carolina Seghini. *Composites Part B: Engineering*[J], 2018, 132: 77
- 2 Xing Dan, Xi Xiongyu, Ma Pengcheng. *Composites Part A: Applied Science and Manufacturing*[J], 2019, 119: 127
- 3 Ying Shuni, Zhou Xiaodong. *Journal of Wuhan University of Technology, Materials Science Edition*[J], 2013, 28: 560
- 4 Davies P, Verbouwe W. *Applied Composite Materials*[J], 2018, 25: 299
- 5 Abraham Brainard C, Nathan Boobesh V, Rajesh Jaipaul S et al. *Materials Today: Proceedings*[J], 2020, 21(1): 380
- 6 Si Jiwen, Li Ziyang, Wang Jingyao et al. *Journal of Non-Crystalline Solids*[J], 2021, 568: 120 941
- 7 Danilo Marini, Marco Valente. *Materials*[J], 2019, 12(18): 2960
- 8 Karonis Dimitrios. *Revista Técnica de la Facultad de Ingeniería Universidad del Zulia*[J], 2014, 37(2): 56
- 9 Ezhil Vannan S, Paul Vizhian S, Karthigeyan R. *Procedia Engineering*[J], 2014, 97: 432
- 10 Karthigeyan R, Ranganath G, Sankaranarayanan S. *European Journal of Scientific Research*[J], 2012, 68(4): 606
- 11 Xie Yuling, Wang Mingliang, Ma Naiheng et al. *Foundry Technology*[J], 2013, 34(7): 803 (in Chinese)
- 12 Onuh Adole, Nilam Barekar, Lorna Anguilano et al. *Materials Letters*[J], 2019, 239: 128
- 13 Li Guobin, Sun Jibing, Guo Quanmei et al. *Journal of Materials Processing Technology*[J], 2005, 161(3): 445
- 14 Overkamp Tim, Mahltig Boris, Kyosev Yordan. *Journal of Industrial Textiles*[J], 2018, 47(5): 815
- 15 Akhlaghi F, Eslami Farsani R, Sabet SMM. *Journal of Composite Materials*[J], 2013, 47(27): 3379
- 16 Ding Hao, Cui Xiping, Xu Changshou et al. *Acta Metallurgica Sinica*[J], 2018, 54(8): 1171 (in Chinese)
- 17 Yang Zhiming, Liu Jinxu, Feng Xinya et al. *Journal of Composite Materials*[J], 2018, 52(14): 1907
- 18 Daoud A. *Materials Science and Engineering A*[J], 2005, 391(1-2): 114
- 19 Wu Gaohui, Zhang Yunhe, Kang Pengchao. *Rare Metal Materials and Engineering*[J], 2007, 36(S3): 328 (in Chinese)
- 20 Zhang Junjia, Jie Jinchuan, Lu Yiping et al. *Journal of Materials Research and Technology*[J], 2021, 11: 197
- 21 Liu Jiaming, Zhang Yubo, Wang Wei et al. *Materials Science and Engineering A*[J], 2022, 831: 142 040
- 22 Gao Meilian, Gao Pingping, Wang Yu et al. *Metals and Materials International*[J], 2021, 27(12): 5425
- 23 Zhang Zhifei, Bai Yang, He Yi et al. *Journal of Materials Science: Materials in Electronics*[J], 2021, 32: 26 412
- 24 Subhasish Sarkar, Rishav Kumar Baranwal, Chanchal Biswas et

- al. *Materials Research Express*[J], 2019, 6(4): 46 415
- 25 Akira Takeuchi, Akihisa Inoue. *Materials Transactions*[J], 2005, 46(12): 2817
- 26 Yang X, Zhang Y. *Materials Chemistry and Physics*[J], 2012, 132(2-3): 233

Ni-Co-P 中间层优化玄武岩纤维增强铝基复合材料的界面结构和力学性能

高昌琦^{1,2}, 马 勤^{1,2,3}, 魏玉鹏^{1,2}, 田江霞^{1,2}, 王乔博^{1,2}, 魏明宇^{1,2}, 任小虎^{1,2}, 丁育胜^{1,2}

(1. 兰州理工大学 省部共建有色金属先进加工与再利用国家重点实验室, 甘肃 兰州 730050)

(2. 兰州理工大学 材料科学与工程学院, 甘肃 兰州 730050)

(3. 泉州信息工程学院 机械与电气工程学院, 福建 泉州 362000)

摘 要: 界面优化是提高铝基复合材料最为有效的手段。通过化学镀工艺成功制备0.2 μm厚Ni-Co-P合金镀层修饰的玄武岩纤维, 并通过真空热压烧结工艺合成Ni-Co-P镀层修饰玄武岩纤维增强2024Al复合材料 (BF(Ni-Co-P)/Al)。探究了Ni-Co-P镀层对BF(Ni-Co-P)/Al复合材料界面结构及拉伸性能的影响机制。结果表明: 复合材料中Ni-Co-P镀层形成稳定的Ni-Co-P中间层, 不仅抑制了玄武岩纤维与铝合金基体间的有害界面反应, 且优化了二者间的结合强度。BF(Ni-Co-P)/Al复合材料密度及硬度明显优于BF/Al复合材料, 且当玄武岩纤维体积分数为30vol%时, BF(Ni-Co-P)/Al复合材料屈服强度和抗拉伸强度分别为252和360 MPa, 大幅高于未修饰纤维增强铝基复合材料和铝合金基体, 并表现出渐进累积失效的断裂模式。

关键词: Ni-Co-P镀层修饰玄武岩纤维; Al基复合材料; 界面结构; 力学性能

作者简介: 高昌琦, 男, 1990年生, 博士生, 兰州理工大学材料科学与工程学院, 甘肃 兰州 730050, E-mail: gaocqlut@sina.com